International Journal of Engineering & Applied Sciences (IJEAS)

Vol.6, Issue 3(2014)52-74

3D elasticity solution for the static analysis of variable thickness bi-directional functionally graded circular plates subjected to non-uniform asymmetric boundary conditions

A.Behravan Rad [a*], *K. Mohammadi Majd* [b]

[a] Department of Mechanical Engineering, Karaj Branch, Islamic Azad University, Karaj, Iran
[b] Engineering Department, Zamyad co, 15 km Karaj old road, P.O 1386183741, Tehran, Iran
[*] *E-mail address*: behravanrad@gmail.com

Abstract

This paper investigates the static behavior of non-uniform bi-directional functionally graded (FG) circular plates embedded on gradient elastic foundations (Winkler- Pasternak type) and subjected to non-uniform asymmetric transverse and in-plane shear loads. The governing state equations are derived in terms of displacements based on 3D theory of elasticity, and assuming the material properties of the plate except the Poisson's ratio varies continuously throughout the thickness and radial directions according to an exponential function. These equations are solved by means semi-analytical method using state-space based differential quadrature method. Numerical results are displayed to clarify the effects of foundation stiffnesses, material heterogeneity indices, various foundation patterns, foundation grading indices, loads ratio and geometric parameters on the displacement and stress fields. The results are reported for the first time and the new results can be used as a benchmark solution for future researches.

Keywords: Functionally graded, circular Plate, Gradient elastic foundation, Elasticity, Semi-analytical method, Boundary condition.

1. Introduction

Recently, a new class of materials known as two-directional functionally graded materials (2D-FGMs) has been introduced in the literature. FGMs have received considerable attention by researchers in recent years because their novel thermo-mechanical properties enable them to be widely used in many scientific and engineering disciplines, such as optics, aerospace, biomedical, civil, mechanical, nuclear and vehicle engineering. Circular plates made of FGMs resting on elastic foundations often find various applications in engineering fields. Typical examples may be found in the power transmission systems, machining devises, photographic facilities, support tables, driven plates of a friction clutch, Vehicle brake disk on friction pads, Nano-plates embedded in an elastic matrix. The bending, vibration, stability and buckling response of such structures to mechanical and thermal loads, with/without considering the interaction between structure-foundation have also been studied by many scientists and numerous papers have been devoted to these problems. Nemat-Alla [1] introduced the concept of adding a third material constituent to the conventional FGMs material in order to significantly reduce the thermal stresses in machine elements that subjected to sever thermal loading, and his investigation on 2D-FGMs has shown that it is more capable of reducing thermal and residual stresses than one-directional FGMs.

A number of approaches have been employed to study the static bending problems of FGM circular plates, among which analytical methods based on certain simplified plate theories have been used frequently. For example, Saidi et al. [2] studied axisymmetric bending of thick functionally graded circular plates based on third order shear deformation plate theory. They

obtained closed form expressions for stress, deflection and moment distribution through the plate and considered various types of boundary conditions for outer edge of the plate. Nosier and Fallah [3] presented analytical solutions for axisymmetric and asymmetric large deformations of FG circular plates under transverse mechanical load based on the first-order shear deformation plate theory with Von Karman non-linearity. Sahraee and Saidi [4] applied fourth order shear deformation plate theory and established four coupled ordinary differential equations to analyze bending and stretching of thick FG plates under the effect of uniformly distributed mechanical load.

Differential quadrature (DQ) method as an efficient and accurate numerical tool has been used to study the static and dynamic behavior of FG circular plates under various loads. Based on the first order shear deformation theory (FSDT) and adopting this technique, Malekzadeh et al. [5] studied the free vibration of temperature-dependent functionally graded annular plates on elastic foundations. Following uncoupled 2D thermo-elasticity theory and virtual work principle, Safaeian et al. [6] presented the effects of thermal environment and temperature-dependence of material properties on axisymmetric bending of FG circular and annular plates. They used the DQ method to obtain the initial thermal stresses and response of the plate. Based on classical plate theory (CPT), Kumar and Lal [7] predicted the free axisymmetric vibration of two directional functionally graded annular plates resting on Winkler foundation using DQ method and Chebyshev collocation technique. In their study power low type property distribution in both thickness and radial directions is considered.

The differential transformation method (DTM) based on the Taylor series expansion is one of the mathematical techniques has been used to solve the differential equation of structures in recent years. Based on classical plate theory and using this method, Shariyat and Alipour [8] analyzed the free vibration and modal stress of two-directional functionally graded circular plates embedded on two-parameter elastic foundations. The static behavior of FG circular plates with power law distribution of constituents and resting on Winkler-type elastic foundation were studied by Abbasi et al. [9].

There are relatively few exact analytical solutions derived directly based on elasticity theory by the researchers, which can serve as benchmarks for accessing the validity of various approximate plate theories or numerical methods. In this regard, Li et al. [10] obtained elasticity solutions for transversely isotropic FG circular plates subject to an axisymmetric transverse load in the form of an even order polynomials (e.g., $q r^k$, k is zero or a finite even integer). Using a direct displacement method, Wang et al. [11] investigated the axisymmetric bending of FG circular plates subjected to Bessel function-type transverse loads. Yun et al. [12] also presented an analytical solution for axisymmetric bending of FG circular plates. Recently, Sburlati and Bardella [13] developed a three-dimensional elasticity solution for the bending problem of FG thick circular plates subjected to axisymmetric conditions. Equilibrium equations are described in terms of potential functions based on Plevako's representation. The material properties were varied along the thickness of the plate.

The semi-analytical method is applicable to more complicated problems. This approach employs the state space method (SSM) to express exactly the plate behavior along the thickness direction and the one dimensional differential quadrature (DQ) rule to approximate the radial variations of the parameters. Based on three-dimensional theory of elasticity and adopting this method, Nie and Zhong [14] investigated the axisymmetric bending of 2D-FG circular and

annular plates. Lu et al. [15] analyzed the static behavior of multidirectional FG rectangular plate. Davoodi et al. [16] demonstrated the free vibration problem of multi-directional FG circular and annular plates. Their work covers the effect of different parameters on natural frequencies and corresponding mode shapes. Most recently, one of the authors discussed the static behavior of unidirectional and two directional FG circular plates resting on linear elastic foundations under the effect of axisymmetric transverse load by using this approach [17-18]. In these studies exponential type of constituent distribution in both thickness and radial directions are considered.

In a survey of literature, the authors have found no work on three dimensional static analysis of variable thickness bi-directional functionally graded circular/annular plates supported by gradient elastic foundations and subjected to compound non-uniform asymmetric loads. Hence, present research is devoted to this problem. In this work, the material properties of the plate except the Poisson's ratio (ν) are assumed to be graded in the thickness and radial directions according to an exponential type distribution of constituents. The formulations are based on the three-dimensional theory of elasticity and a hybrid semi-analytical approach, which makes use of the state space method and the one-dimensional differential quadrature rule, is employed to extract the numerical results. A convergence study of the proposed method is performed for non-uniform multi-directional FG circular plates, and its accuracy is validated by comparing the results are available in the open literature. The effects of material properties gradient indices, loads ratio, foundation parameters and plate geometry variation coefficients on the displacement and stress fields are intensively investigated.

The novelties of the present study can be summarized as follow:

- Presenting a semi-analytical solution for static analysis of variable thickness 2D-FG circular/annular plates with complicated boundary conditions.
- Three dimensional deformation and stress analyses of non-uniform 2D-FG circular/annular plates under the effect of general tractions (e.g., variation of mechanical loads and plate-foundation interaction in an arbitrary pattern in the radial and circumferential directions), for the first time.
- Extracting new differential equation for the two parameters linear elastic foundation with gradient coefficients in both radial and circumferential directions, for the first time.
- Presenting the effect of foundation parameters and foundation gradient indices on elastic behavior of variable thickness 2D-FG circular/annular plates, for the first time.
- Presenting quite new and interesting stress and deformation results for the non-uniform 2D-FG circular/annular plates.

2. Problem formulation

2.1 Basic equations

Fig.1 illustrates a non-uniform bi-directional functionally graded annular plate with outer radius a, inner radius b, inner edge thickness h_o embedded on gradient elastic foundation and subjected to combined non-uniform asymmetric transverse and in-plane shear loads. To describe the displacement field of the plate an orthogonal cylindrical coordinate system (r, θ, z) with the origin o located at the center of mid surface of the plate is used.

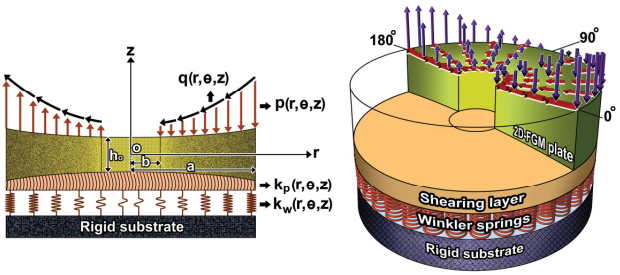

Fig. 1 Geometry of non-uniform 2D-FGMs annular plate resting on gradient elastic foundations

To demonstrate the plate material properties, geometry of the plate, external asymmetric loads the fallowing equations are considered.

$$E(r,z)=E_b\exp\left(n_1\left(\frac{z}{h}+\frac{1}{2}\right)+n_2\left(\frac{r-b}{a-b}\right)\right) \tag{1}$$

$$h(r)=\frac{h_o}{2}\left(1+\alpha_1\left(\frac{r-b}{a-b}\right)+\alpha_2\left(\frac{r-b}{a-b}\right)^2\right) \tag{2}$$

$$p(r,\theta,z)=p_o\left(1+p_1\left(\frac{r-b}{a-b}\right)+p_2\left(\frac{r-b}{a-b}\right)^2\right)\cos(\theta) \tag{3}$$

$$q(r,\theta,z)=q_o\left(1+q_1\left(\frac{r-b}{a-b}\right)+q_2\left(\frac{r-b}{a-b}\right)^2\right)\cos(\theta) \tag{4}$$

where E_b is the Young's module at the bottom surface and inner radius of the plate, n_1, n_2 are the parameters indicating the trends of the plate material properties gradient, p_o, q_o are the values of external loads at the inner radius of the plate, $\alpha_1,\alpha_2,p_1,p_2,q_1,q_2$ are the plate geometry and external loads variation coefficients.

In the absence of body forces the equilibrium equations are

$$\sigma_{r,r}+r^{-1}\tau_{r\theta,\theta}+\tau_{rz,z}+r^{-1}(\sigma_r-\sigma_\theta)=0 \tag{5-a}$$

$$\tau_{r\theta,r}+r^{-1}\sigma_{\theta,\theta}+\tau_{\theta z,z}+2r^{-1}\tau_{r\theta}=0 \tag{5-b}$$

$$\tau_{rz,r}+r^{-1}\tau_{\theta z,\theta}+\sigma_{z,z}+r^{-1}\tau_{rz}=0 \tag{5-c}$$

where $\sigma_r,\sigma_\theta,\sigma_z,\tau_{\theta z},\tau_{rz},\tau_{r\theta}$ are the stress components and the comma denotes differentiation with respect to the indicated variable.

The displacements field is

$$u(r,\theta,z)=u(r,z)\cos(\theta) \tag{6-a}$$

$$v(r,\theta,z)=v(r,z)\sin(\theta) \tag{6-b}$$

$$w(r,\theta,z)=w(r,z)\cos(\theta) \tag{6-c}$$

where u,v,w are displacement components in the r,θ and z directions.

The kinematic equations are

$$\varepsilon_r=u(r,\theta,z)_{,r} \tag{7-a}$$

$$\varepsilon_\theta=r^{-1}v(r,\theta,z)_{,\theta}+r^{-1}u \tag{7-b}$$

$$\varepsilon_z=w(r,\theta,z)_{,z} \tag{7-c}$$

$$\gamma_{rz}=u(r,\theta,z)_{,z}+w(r,\theta,z)_{,r} \tag{7-d}$$

$$\gamma_{\theta z}=r^{-1}w(r,\theta,z)_{,\theta}+v(r,\theta,z)_{,z} \qquad (7\text{-e}) \qquad \gamma_{r\theta}=r^{-1}u(r,\theta,z)_{,\theta}+v(r,\theta,z)_{,r}-r^{-1}v(r,\theta,z) \qquad (7\text{-f})$$

where $\varepsilon_r, \varepsilon_\theta, \varepsilon_z, \gamma_{\theta z}, \gamma_{rz}, \gamma_{r\theta}$ are the strain components.

The constitutive relations from 3-D theory of elasticity are

$$\sigma_r=\frac{E(r,z)}{(1+\nu)(1-2\nu)}\Big((1-\nu)\,u(r,\theta,z)_{,r}+\nu\, r^{-1}\,(v(r,\theta,z)_{,\theta}+u(r,\theta,z))+\nu\, w(r,\theta,z)_{,z}\Big) \qquad (8\text{-a})$$

$$\sigma_\theta=\frac{E(r,z)}{(1+\nu)(1-2\nu)}\Big(\nu\, u(r,\theta,z)_{,r}+(1-\nu)\,r^{-1}\,u(r,\theta,z)+\nu\, w(r,\theta,z)_{,z}\Big) \qquad (8\text{-b})$$

$$\sigma_z=\frac{E(r,z)}{(1+\nu)(1-2\nu)}\Big(\nu\, u(r,\theta,z)_{,r}+\nu\, r^{-1}\,u(r,\theta,z)+(1-\nu)\,w(r,\theta,z)_{,z}\Big) \qquad (8\text{-c})$$

$$\tau_{rz}=\frac{E(r,z)}{2(1+\nu)}\Big(u(r,\theta,z)_{,z}+w(r,\theta,z)_{,r}\Big) \qquad (8\text{-d})$$

$$\tau_{\theta z}=\frac{E(r,z)}{2(1+\nu)}\Big(r^{-1}\,w(r,\theta,z)_{,\theta}+v(r,\theta,z)_{,z}\Big) \qquad (8\text{-e})$$

$$\tau_{r\theta}=\frac{E(r,z)}{2(1+\nu)}\Big(v(r,\theta,z)_{,r}-r^{-1}\,v(r,\theta,z)+r^{-1}\,u(r,\theta,z)_{,\theta}\Big) \qquad (8\text{-f})$$

For the sake of dimensionless formulae, the following non-dimensional quantities are introduced:

$$U=\frac{u(r,\theta,z)}{h(r)}\ ,\ V=\frac{v(r,\theta,z)}{h(r)}\ ,W=\frac{w(r,\theta,z)}{h(r)},\ \eta=\frac{r}{a}\ ,\xi=\frac{z(r)}{h(r)},\ s=\frac{h_o}{2a}\ ,-0.5\le\xi\le 0.5\,,\ \zeta=\xi+0.5$$
$$\sigma_\eta=\frac{\sigma_r}{p},\ \sigma_\Theta=\frac{\sigma_\theta}{p},\ \sigma_\xi=\frac{\sigma_z}{p},\ \tau_{\eta\xi}=\frac{\tau_{rz}}{p},\ \ \tau_{\Theta\xi}=\frac{\tau_{\theta z}}{p},\ \ \ \tau_{\eta\Theta}=\frac{\tau_{r\theta}}{p} \qquad (9)$$

by considering the Eqs.(1)-(9), the normalized form of the governing differential equations in terms of displacements in the bottom surface of the plate can be obtained as:

$$\begin{aligned}U_{,\zeta\zeta}=&-\left(\frac{2(1-\nu)}{1-2\nu}\right)(s)^2\beta_1^2\left(U_{,\eta\eta}+\left(\frac{1}{\eta}+\frac{n_2}{1-b/a}+2\beta_2\right)U_{,\eta}+\left(\left(\frac{1}{\eta}+\frac{n_2}{1-b/a}\right)\beta_2+\beta_3-\frac{1}{\eta^2}\right)U\right)\\
&-\left(\frac{2\nu}{1-2\nu}\right)(s)^2\beta_1^2\,\frac{n_2}{\eta(1-b/a)}U+(s)^2\beta_1^2\frac{1}{\eta^2}U-\frac{2\nu}{1-2\nu}(s)^2\beta_1^2\frac{1}{\eta}\left(V_{,\eta}+\left(\beta_2+\frac{n_2}{1-b/a}\right)V\right)+\frac{2(1-\nu)}{1-2\nu}(s)^2\beta_1^2\frac{V}{\eta^2}\\
&-(s)^2\beta_1^2\left(\frac{1}{\eta}V_{,\eta}+\left(\frac{\beta_2}{\eta}-\frac{1}{\eta^2}\right)V\right)-n_1 s\beta_1\left(W_{,\eta}+\beta_2 W\right)-n_1\,U_{,\zeta}\\
&-\left(\frac{2\nu}{1-2\nu}\right)s\beta_1\left(W_{,\eta\zeta}+\left(\beta_2+\frac{n_2}{1-b/a}+\frac{1}{\eta}\right)W_{,\zeta}\right)+\left(\frac{2\nu}{(1-2\nu)}\right)\frac{s\beta_1}{\eta}\,W_{,\zeta}-s\beta_1\left(W_{,\eta\zeta}+\beta_2 W_{,\zeta}\right)\end{aligned} \qquad (10\text{-a})$$

$$V_{,\zeta\zeta}=\frac{2\nu}{1-2\nu}(s)^2\frac{\beta_1^2}{\eta}\left(U_{,\eta}+\beta_2 U\right)+\frac{2(1-\nu)}{(1-2\nu)}(s)^2\beta_1^2\frac{U}{\eta^2}+(s)^2\beta_1^2\left(\frac{1}{\eta}U_{,\eta}+\left(\frac{1}{\eta}\left(\beta_2+\frac{n_2}{1-b/a}\right)+\frac{U}{\eta^2}\right)\right)$$
$$+\frac{2(1-\nu)}{(1-2\nu)}(s)^2\beta_1^2\frac{V}{\eta^2}-(s)^2\beta_1^2\left(V_{,\eta\eta}+\left(2\beta_2+\frac{1}{\eta}+\frac{n_2}{1-b/a}\right)V_{,\eta}+\left(\beta_2+\beta_3+\left(\beta_2-\frac{1}{\eta}\right)\left(\frac{n_2}{1-b/a}\right)-\frac{1}{\eta^2}\right)V\right) \qquad (10\text{-b})$$
$$+n_1 s\beta_1\frac{W}{\eta}-n_1 V_{,\zeta}+\frac{1}{\eta}\left(\frac{1}{1-2\nu}\right)W_{,\zeta}$$

$$
\begin{aligned}
W_{,\zeta\zeta} &= -n_1\left(\frac{\nu}{1-\nu}\right)s\beta_1\left(U_{,\eta}+\left(\beta_2+\frac{1}{\eta}\right)U\right)-n_1\left(\frac{\nu}{1-\nu}\right)s\beta_1\frac{V}{\eta}\\
&+\left(\frac{1-2\nu}{2(1-\nu)}\right)s^2\beta_1^2\left(W_{,\eta\eta}+\left(\frac{1}{\eta}+2\beta_2+\frac{n_2}{1-b/a}\right)W_{,\eta}+\left(\beta_3+\beta_2\left(\frac{1}{\eta}+\frac{n_2}{1-b/a}\right)\right)W\right)\\
&-\left(\frac{\nu}{(1-\nu)}\right)s\beta_1\left(U_{,\eta\zeta}+\left(\beta_2+\frac{1}{\eta}\right)\frac{1}{\eta}U_{,\zeta}\right)-\left(\frac{1-2\nu}{2(1-\nu)}\right)s\beta_1\left(\frac{n_2}{1-b/a}\right)U_{,\zeta}-\frac{1}{2(1-\nu)}s\beta_1\frac{V_{,\zeta}}{\eta}-n_1W_{,\zeta}
\end{aligned}
\tag{10-c}
$$

where

$$
\beta_1=\left(1+\alpha_1\left(\frac{\eta-b/a}{1-b/a}\right)+\alpha_2\left(\frac{\eta-b/a}{1-b/a}\right)^2\right),\ \beta_2=\frac{1}{(1-b/a)}\left(\alpha_1+2\alpha_2\left(\frac{\eta-b/a}{1-b/a}\right)\right)\Big/\beta_1\ ,\ \beta_3=2\alpha_2/\beta_1(1-b/a)^2
$$

2.2 The plate-foundation interaction

It is assumed that, the two parameter elastic foundation is perfect, frictionless, attached to the plate, non-uniform, asymmetric, and isotropic, that is, $k_{pr}=k_{p\theta}=k_p$. In the referred coordinate system the interface pressure p_{zb} between the structure and a non-uniform foundation may be expressed mathematically as follow

$$
p_{zb}=k_w(r,\theta,z)w_b-\frac{1}{r}\frac{\partial}{\partial r}(r\,k_p(r,\theta,z)\frac{\partial w_b}{\partial r})-\frac{1}{r^2}\frac{\partial}{\partial\theta}(k_p(r,\theta,z)\frac{\partial w_b}{\partial\theta})
\tag{11}
$$

where p_{zb} denotes the foundation reaction per unit area and w_b is the deflection of the bottom surface of the plate. $k_w(r,\theta,z)$, $k_p(r,\theta,z)$ are the coordinate dependent Winkler-Pasternak coefficients and can be expressed as

$$
k_w(r,\theta,z)=k_{wbo}\left(1+f_1(r/a)+f_2(r/a)^2\right)\cos(\theta)\ ,\ k_p(r,\theta,z)=k_{Pbo}\left(1+f_1(r/a)+f_2(r/a)^2\right)\cos(\theta)
\tag{12}
$$

where $k_{wbo}(N/m^3)$, $k_{pbo}(N/m)$ are the elastic coefficients of Winkler-Pasternak foundation at the center of bottom surface of the plate

2.3 Boundary and edge conditions

The edge conditions for solid circular plate ($b=0$) are

Clamped edge (C):

$$
u(r,\theta,z)=0,\quad v(r,\theta,z)=0,\quad w(r,\theta,z)=0 \qquad \text{at}\quad r=a
\tag{13}
$$

Simply supported edge (S):

$$
\sigma_r=0,\quad v(r,\theta,z)=0,\quad w(r,\theta,z)=0 \qquad \text{at}\quad r=a
\tag{14}
$$

Free edge (F):

$$
\sigma_r=0,\quad \tau_{r\theta}=0,\quad \tau_{rz}=0 \qquad \text{at}\quad r=a
\tag{15}
$$

Regularity conditions on the center of the plate:

$$
u(r,\theta,z)=0,\quad v(r,\theta,z)=0,\quad w(r,\theta,z)_{,r}=0 \qquad \text{at}\quad r=0
\tag{16}
$$

The edge conditions for annular plate are

Clamped – clamped edges (C-C):

$$
u(r,\theta,z)=0,\quad v(r,\theta,z)=0,\quad w(r,\theta,z)=0 \qquad \text{at}\quad r=b
\tag{17-a}
$$

$$
u(r,\theta,z)=0,\quad v(r,\theta,z)=0,\quad w(r,\theta,z)=0 \qquad \text{at}\quad r=a
\tag{17-b}
$$

Simply – simply supported edges (S-S):

$$\sigma_r = 0, \quad v(r,\theta,z) = 0, \quad w(r,\theta,z) = 0 \qquad \text{at} \quad r = b \tag{18-a}$$

$$\sigma_r = 0, \quad v(r,\theta,z) = 0, \quad w(r,\theta,z) = 0 \qquad \text{at} \quad r = a \tag{18-b}$$

Simply supported – clamped edges (S-C):

$$\sigma_r = 0, \quad v(r,\theta,z) = 0, \quad w(r,\theta,z) = 0 \qquad \text{at} \quad r = b \tag{19-a}$$

$$u(r,\theta,z) = 0, \quad v(r,\theta,z) = 0, \quad w(r,\theta,z) = 0 \qquad \text{at} \quad r = a \tag{19-b}$$

Clamped – free edges (C-F):

$$u(r,\theta,z) = 0, \quad v(r,\theta,z) = 0, \quad w(r,\theta,z) = 0 \qquad \text{at} \quad r = b \tag{20-a}$$

$$\sigma_r = 0, \quad \tau_{r\theta} = 0, \quad \tau_{rz} = 0 \qquad \text{at} \quad r = a \tag{20-b}$$

Boundary conditions at the top and bottom surfaces of the plate are assumed as follow:

at $z = -h/2$,

$$\sigma_z = p_{zb} \quad , \quad \tau_{z\theta} = 0 \quad , \quad \tau_{rz} = 0 \tag{21}$$

at $z = h/2$,

$$\sigma_z = -p(r,\theta,z) \quad , \quad \tau_{z\theta} = 0 \quad , \quad \tau_{rz} = -q(r,\theta,z) \tag{22}$$

3. Solution technique

Obtaining an analytical solution for the governing differential equations appeared in Eq. (10) is difficult, if it is not impossible. Hence, a semi-analytical procedure is employed in this study. This method gives an analytical solution along the thickness direction (z-direction) by using the state space method (SSM) and a numerical solution in the radial direction of the plate by applying one dimensional differential quadrature rule (DQ) to approximate the stress and deformation fields. By using this method the governing differential equations is transformed from physical domain to a normalized computational domain and the special derivatives are discretized by applying the one dimensional differential quadrature rule as an efficient and accurate numerical tool. The obtained linear eigenvalue system in terms of the displacements is solved and the static behavior of the plate under non-uniform boundary conditions is analyzed.

3.1 DQM procedure and its application

The DQ method is a numerical technique which divides the continuous domain in to a set of discrete points and replaces the derivative of an arbitrary unknown function with the weighted summation of the functions values in the discretized points. There for, the principle of DQ rule can be stated as follow: for a continuous function $g(r)$ defined in an interval $r \in [0,1]$, its nth-order derivative with respect to argument r at an arbitrary given point r_i can be approximated by a linear sum of the weighted function values of $g(r)$ in the whole domain [19, 20]. The mathematical presentation of the method is

$$\frac{\partial^{(n)} g(r_i)}{\partial r^n} = \sum_{j=1}^{N} A_{ij}^{(n)} g(r_j) \qquad i = 1,2,\cdots,N \quad \text{and} \quad n = 1,2,\cdots,N-1 \tag{23}$$

where $A_{ij}^{(n)}$ is the weighting coefficients matrix of the nth-derivative determined by the coordinates of the sample points r_i and N is the number of the grid points in the radial direction.

There are different ways for calculating the weighting coefficient matrix, because different

functions may be considered as test functions. In this study a set of Lagrange polynomials are employed as test functions, and to achieve more accuracy the non-uniform grid spacing is considered. Explicit expressions of the first and second derivatives of the weighted coefficients matrices and also criterion to adopt non-uniformly spaced grid points are [19, 20]:

1) - The first order derivative of the weighting coefficients matrix

$$A_{ik}=\frac{\prod_{j=1,j\neq i}^{N}(r_i-r_j)}{(r_i-r_k)\prod_{j=1,j\neq k}^{N}(r_k-r_j)} \qquad i\neq k\,,\ \ i,k=1,2,3,\cdots,N$$

$$A_{ii}=-\sum_{j=1,j=i}^{N}A_{ij} \qquad i=k\,, \qquad i=1,2,3,\cdots,N$$

(24)

2) - The second-order derivative of the weighting coefficients matrix

$$A_{ik}^{(2)}=2\left[A_{ii}A_{ik}-\frac{A_{ik}}{r_i-r_k}\right] \qquad i\neq k\,,\ \ i,k=1,2,3,\cdots,N$$

$$A_{ii}^{(2)}=-\sum_{j=1,j=i}^{N}A_{ij}^{(2)} \qquad i=k\,, \qquad i=1,2,3,\cdots,N$$

(25)

3) - The Chebyshev-Gauss-Lobatto criterion

$$r_i=\frac{1}{2}\left[1-\cos\left(\frac{(i-1)\pi}{N-1}\right)\right](a-b)+b \qquad i=1,2,3,\cdots,N \qquad (26)$$

The partial derivatives of the unknown displacements U,V,W with respect to η appeared in Eq. (10) after applying the DQ rule at an arbitrary sample point η_i can be expressed as:

$$\left(U,\eta\right)_{\eta i}=\sum_{j=1}^{N}A_{ij}U_j \qquad (27\text{-a}) \qquad \left(V,\eta\right)_{\eta i}=\sum_{j=1}^{N}A_{ij}V_j \qquad (27\text{-b})$$

$$\left(W,\eta\right)_{\eta i}=\sum_{j=1}^{N}A_{ij}W_j \qquad (27\text{-c}) \qquad \left(U,\eta\eta\right)_{\eta i}=\sum_{j=1}^{N}A_{ij}^{(2)}U_j \qquad (27\text{-d})$$

$$\left(V,\eta\eta\right)_{\eta i}=\sum_{j=1}^{N}A_{ij}^{(2)}V_j \qquad (27\text{-e}) \qquad \left(W,\eta\eta\right)_{\eta i}=\sum_{j=1}^{N}A_{ij}^{(2)}W_j \qquad (27\text{-f})$$

$$\left(U,\eta\zeta\right)_{\eta i}=\sum_{j=1}^{N}A_{ij}\,U_{,\zeta j} \qquad (27\text{-g}) \qquad \left(V,\eta\zeta\right)_{\eta i}=\sum_{j=1}^{N}A_{ij}\,V_{,\zeta j} \qquad (27\text{-h})$$

$$\left(W,\eta\zeta\right)_{\eta i}=\sum_{j=1}^{N}A_{ij}W_{,\zeta j} \qquad (27\text{-i})$$

The associated edge conditions in discretized points can be written as follows:

Clamped edge (C):

$$U_N=0\,,\quad V_N=0,\quad W_N=0 \qquad \text{at}\ \ \eta=1 \qquad (28)$$

Simply- supported edge (S):

$$\sigma_{\eta N}=0\ \ ,\ \ V_N=0\ \ ,\ \ W_N=0 \qquad \text{at}\ \ \eta=1 \qquad (29)$$

Free edge (F):

$$\sigma_{\eta N}=0\ \ ,\ \ \tau_{\eta\Theta N}=0\ \ ,\ \ \tau_{\eta\xi N}=0 \qquad \text{at}\ \ \eta=1 \qquad (30)$$

Regularity conditions on the center of the plate:

$$U_1 = 0\,,\ V_1 = 0\,,\ W_1 = -\sum_{j=2}^{N} \frac{A_{1j}}{(\beta_{21} + A_{11})} W_j \quad \text{at} \quad \eta = 0 \tag{31}$$

Clamped – clamped edges (C-C):

$$U_1 = 0\,,\quad V_1 = 0\quad ,\quad W_1 = 0 \qquad \text{at} \quad \eta = b/a \tag{32-a}$$

$$U_N = 0\,,\quad V_N = 0\quad ,\quad W_N = 0 \qquad \text{at} \quad \eta = 1 \tag{32-b}$$

Simply – simply supported edges (S-S):

$$\sigma_{\eta 1} = 0\,,\quad V_1 = 0,\quad W_1 = 0 \qquad \text{at} \quad \eta = b/a \tag{33-a}$$

$$\sigma_{\eta N} = 0\,,\quad V_N = 0,\quad W_N = 0 \qquad \text{at} \quad \eta = 1 \tag{33-b}$$

Simply supported – clamped edges (S-C):

$$\sigma_{\eta 1} = 0\,,\quad V_1 = 0,\quad W_1 = 0 \qquad \text{at} \quad \eta = b/a \tag{34-a}$$

$$U_N = 0\,,\quad V_N = 0\quad ,\quad W_N = 0 \qquad \text{at}\ \eta = 1 \tag{34-b}$$

Clamped – free edges (C-F):

$$U_1 = 0\,,\quad V_1 = 0\quad ,\quad W_1 = 0 \qquad \text{at} \quad \eta = b/a \tag{35-a}$$

$$\sigma_{\eta N} = 0\quad ,\quad \tau_{\eta \Theta N} = 0\quad ,\quad \tau_{\eta \xi N} = 0 \quad \text{at} \quad \eta = 1 \tag{35-b}$$

The discretized forms of the boundary conditions at the lower and upper surfaces of the plate, Eqs.(21) and (22) can be written as

At $\zeta = 0$,

$$\left(U,\zeta\right)_i + s\beta_{1i}\left(\sum_{j=1}^{N} A_{ij} W_j + \beta_{2i} W_i\right) = 0 \tag{36-a}$$

$$\left(V,\zeta\right)_i - s\,\frac{\beta_{1i}\cot g(\theta)}{\eta_i} W_i = 0 \tag{36-b}$$

$$\left(W,\zeta\right)_i + \frac{s\nu}{1-\nu}\beta_{1i}\left(\sum_{j=1}^{N} A_{ij} U_j + \left(\beta_{2i} + \frac{1}{\eta_i}\right) U_i + \frac{tg(\theta)}{\eta_i}\, V_i\right) =$$

$$\frac{\beta_{1i}}{\exp\left(n_2\left(\dfrac{\eta_i - b/a}{1 - b/a}\right)\right)}\left(k_1 \beta_{4i}\cos(\theta) W_{bi} - k_2\left(\begin{array}{l}\beta_{4i}\cos(\theta)\displaystyle\sum_{j=1}^{N} A_{ij}^{(2)} W_{bj} + \left(2\beta_{2i}\beta_{4i} + \dfrac{\beta_{4i}}{\eta_i} + \beta_{5i}\right)\cos(\theta)\sum_{j=1}^{N} A_{ij} W_{bj} + \\ \left(\left(\beta_{2i}\left(\dfrac{\beta_{4i}}{\eta_i} + \beta_{5i}\right) + \beta_{3i}\beta_{4i}\right)\cos(\theta) + \right. \\ \left.\left(\beta_{4i}\left(\cos^2(\theta) - \sin^2(\theta)\right)\right)\dfrac{1}{\eta_i^2}\right) W_{bi}\end{array}\right)$$

$$(i = 1,2,3,\ldots,N) \tag{36-c}$$

where $k_1=\frac{k_{wb0}(1+\nu)(1-2\nu)h}{2(1-\nu)E_b}$, $k_2=\frac{k_{pbo}(1+\nu)(1-2\nu)}{2(1-\nu)E_b}\frac{s}{a}$ are the dimensionless coefficients of the elastic foundation and $\beta_{4i}=\left(1+f_1\eta_i+f_2\eta_i^2\right)$, $\beta_{5i}=\left(f_1+2f_2\eta_i\right)$.

At $\zeta=1$,

$$\left(U,\zeta\right)_i+s\beta_{1i}\left(\sum_{j=1}^{N}A_{ij}W_j+\beta_{2i}W_i\right)=\frac{-2(1+\nu)q_i}{\exp\left(n_1+n_2\left(\frac{\eta_i-b/a}{1-b/a}\right)\right)} \tag{37-a}$$

$$\left(V,\zeta\right)_i-s\frac{\beta_{1i}\cot g(\theta)}{\eta_i}W_i=0 \tag{37-b}$$

$$\left(W,\zeta\right)_i+\frac{s\nu}{(1-\nu)}\beta_{1i}\left(\sum_{j=1}^{N}A_{ij}U_j+\left(\beta_{2i}+\frac{1}{\eta_i}\right)U_i+\frac{tg(\theta)}{\eta_i}V_i\right)=\frac{-(1+\nu)(1-2\nu)P_i}{(1-\nu)\exp\left(n_1+n_2\left(\frac{\eta_i-b/a}{1-b/a}\right)\right)} \tag{37-c}$$

$$(i=1,2,3,\ldots,N)$$

3.2 The state space method

By taking the elements of state vector as $\delta=\left[U \quad V \quad W \quad U,\zeta \quad V,\zeta \quad W,\zeta\right]^T$, the global state space notation of equations (10) in discretized points can be written as

$$\{\delta_i(\zeta)\}_{,\zeta}=[D_i]\{\delta_i(\zeta)\} \tag{38}$$

Here, $\delta_i(\zeta)=\left[\left[U_i\right] \quad \left[V_i\right] \quad \left[W_i\right] \quad \left[U,\zeta_i\right] \quad \left[V,\zeta_i\right] \quad \left[W,\zeta_i\right]\right]^T$ is the global state vector along the plate thickness at the level of ζ and D_i is the coefficient matrix at the sample points. The elements of matrix D_i are expressed in appendix 1.

By considering all edge conditions the Eq. (38) can be denoted as follow;

$$\left[\delta_{ei}(\zeta)\right]_{,\zeta}=\left[D_{ei}\right]\left[\delta_{ei}(\zeta)\right] \tag{39}$$

where the subscript ‘e’ denotes the modified matrix or unknown vector taking account of the edge conditions.

According to the rules of matrix operation, the general solution to Eq. (39) is:

$$\delta_{ei}(\zeta)=\exp\left(\zeta D_{ei}\right)\delta_{ei}(0) \tag{40}$$

Eq. (40) establishes the transfer relations from the state vector on the bottom surface to that at an arbitrary plane ζ of the plate by the exponential matrix of $\exp\left(\zeta D_{ei}\right)$. Setting $\zeta=1$ in Eq. (40) gives

$$\delta_{ei}(1)=\exp\left(D_{ei}\right)\delta_{ei}(0) \tag{41}$$

where $\exp\left(D_{ei}\right)$ is the global transfer matrix and $\delta_{ei}(1)$, $\delta_{ei}(0)$ are the values of the state variables at the upper and lower planes of the plate, respectively.

By substituting the boundary conditions presented in Eqs.(36) and (37) in to Eq.(41), the following algebraic equations for bending analysis can be obtained

$$MT = Q \tag{42}$$

where M is a 6(N-2)×6(N-2) matrix, Q is a traction force vector and T is:

$$T = \left[\left[U_i(0)\right] \ \left[V_i(0)\right] \ \left[W_i(0)\right] \ \left[U_i(1)\right] \ \left[V_i(1)\right] \ \left[W_i(1)\right]\right]^T \quad ,(i = 2, 3, \cdots, N-1) \tag{43}$$

By solving Eq. (42), all state parameters at $\zeta = 0$, $\zeta = 1$ are obtained. We can use Eqs. (40) and (8) to calculate the displacements and the stresses through the thickness of the FGMs circular plate.

4. The numerical results and discussions

In this section, firstly, the foregoing analysis is verified by comparing numerical results available for a uniform thickness FG circular plate subjected to axisymmetric transverse load has been considered by Li et al. [10], then the convergence of the current solution procedure is conducted to illustrate the efficiency of the present method for a complicated problem and is used as an evaluation criterion. The numerical results are derived for non-uniform thickness2D-FG clamped-clamped annular and clamped circular plates under described loading. The number of non-uniformly spaced discrete points in the radial direction is nine. Finally, effects of the material heterogeneity indices, loads ratio and foundation parameters (e.g., Winkler-Pasternak coefficients and foundation gradient indices) on static behavior of the plates are intensively discussed in the following text. The numerical results are shown in Figs.2-9.

4.1 Validation of the code

Since there are no results available in the open literature for static response of variable thickness 2D-FGMs circular plate to non-uniform boundary conditions, there for the validity of the prepared computer code is investigated by computing the dimensionless transverse shear stress distribution along the plate thickness to a simply- supported FG circular plate under an axisymmetric distributed transverse load without elastic foundation previously considered by Li et al. [10]. The structural parameters and boundary conditions on the bottom and the top surfaces of the plate are considered same as given by reference [10]. Non-dimensional transverse shear stress of the mentioned plate is determined and the results are presented in Fig. 2. It is evident from Fig. 2 that the present results are in good agreement with those are given by Li et al. [10].

In order to extract the new numerical results, non-uniform 2D-FG clamped-clamped annular and clamped circular plates consisting of Titanium $E_T = 110.25\,\text{GPa}$ and Zirconium $E_z = 278.41\,\text{GPa}$ as the metal and ceramic constituents of the plate has been studied earlier by

Yun et al. [12] are considered. The plate structural data and the boundary conditions on the lower and the upper surfaces of the plate are:

$$E_b(b,-h_o/2)=110.25\,\text{GPa}\,,\ E_t(a,h/2)=278.41\,\text{GPa}\,,\ \nu=0.3\,,\ a=1.0\,\text{m}\,,\ s=0.02\,,\ b=0.1\,\text{m}$$

$$\alpha_1=\alpha_2=0.1\,,\ f_1=f_2=0.1\,,\ k_1=k_2=0.1,\ p_1=p_2=q_1=q_2=0.1$$

$$\tau_{rz}=0\,,\ \sigma_z=p_{zb}\,,\ \tau_{\theta z}=0 \quad \text{at } z=-h_o/2 \qquad \tau_{rz}=-1\text{GPa}\,,\ \sigma_z=-1GPa\,,\ \tau_{\theta z}=0 \quad \text{at } z=h_o/2 \quad (44)$$

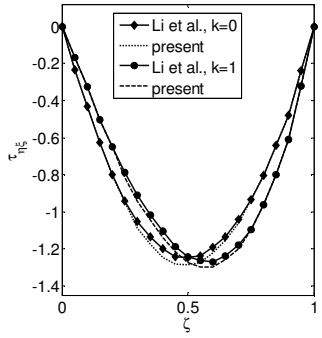

Fig.2 Distribution of dimensionless transverse shear stress across the plate thickness at $\eta=0.5$

Fig.3 depicts the dimensionless transverse deflection W_b versus the number of discrete points N at a location $\eta=0.55,\theta=45^o$ for clamped-clamped supported plate with structural data and boundary conditions shown in Eq. (44), and $n_1=n_2=0.5,1,1.5$ for convex thickness ($\alpha_1=\alpha_2=-0.1$), uniform thickness ($\alpha_1=\alpha_2=0$) and concave thickness ($\alpha_1=\alpha_2=0.1$) respectively. It can be seen from Fig.3 that the dimensionless deflection of the plate approaches to a specific value with an increase in the number of the discretization points. This figure confirms that the convergence of the present method is great.

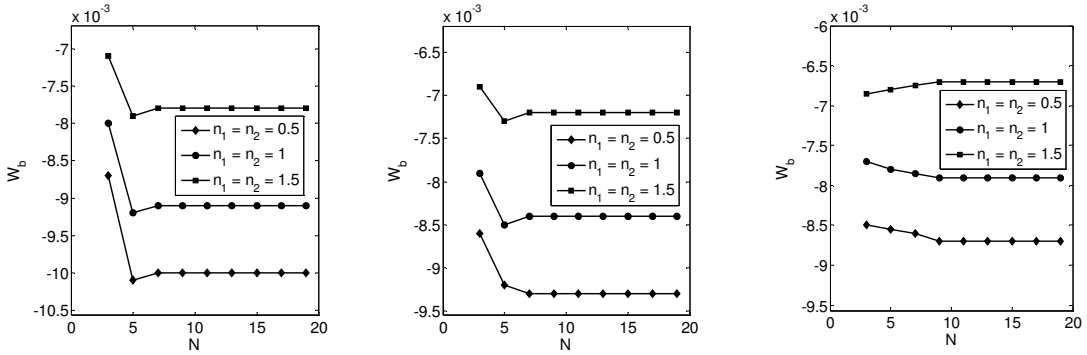

a) Convex thickness **b)** Uniform thickness **c)** Concave thickness

Fig.3 Convergence of non-dimensional deflection of the plate at a location ($\eta=0.55\,,\theta=45^\circ$)

Fig.4 illustrates distribution of the displacement and stress components along the thickness of the plate (C-C supported) at $\eta=0.55,\theta=45^o$ due to conditions discussed in Eq. (44) and gradient indices $n_1=n_2=0.25,0.5,1,1.5$. It can be found from Fig.4 that the U and V displacements decrease, σ_η increases, σ_Θ firstly decreases and then increases, $\sigma_\xi,\tau_{\eta\xi}$ decrease and $\tau_{\theta\xi},\tau_{\eta\theta}$ increase along the thickness of the plate as n_1,n_2 increase. The transverse displacement has complicated behavior it increases with increasing graded indices and decreases

as heterogeneity indices increase for small and large values of n_1 and n_2 respectively. The distribution of $\tau_{\eta\xi}$ and $\tau_{\theta\xi}$ stresses through the thickness of the plate converges to the horizontal line with decreasing the graded indices, which is the characteristic of thin and homogeneous plate. Decrease of displacements indicates that increasing the material heterogeneity indices will certainly enhance the deformation rigidity of the plate.

Fig.5 plots the effect of loads ratio on static response of the plate(C-C supported) at $\eta = 0.55, \theta = 45^o$ with structural parameters discussed in Eq. (44), $n_1 = n_2 = \ln(E_T/E_z)$ and $q_o/p_o = 2,4,6,8$. It is observed from Fig.5 that all displacements and stress components increase as the loads ratio increases. The radial and hoop stresses have increased by additional compression of the layers in the radial direction due to in plane shear interaction, consequently, these stress components through the thickness direction is more affected by the loads ratio variations at both surfaces especially at the upper surface. As Fig.5 (h) shows the stress $\tau_{\theta\xi}$ satisfies the boundary conditions.

Effect of the foundation stiffnesses on static behavior of the plate(C-C supported) whit above mentioned conditions and $n_1 = n_2 = \ln(E_T/E_z)$ at $\eta = 0.97, \theta = 45^o$ is depicted in Fig.6. It can be found from Fig.6 that $U, \sigma_\eta, \sigma_\Theta, \tau_{\theta\xi}$ increase and V, W, σ_ξ, $\tau_{\eta\xi}$, $\tau_{\eta\theta}$ decrease when k_1, k_2 increase.

In the next stage, effect of foundation gradient indices and various patterns of the stiffness variations on mechanical entities along the thickness direction are studied. For this purpose, a clamped circular plate with the geometric and material data discussed in Eq. (44) and $k_1 = k_2 = 0.01$ is considered. The through-the-thickness distributions of the dimensionless displacement and stress components are determined at mid-radius point and $\theta = 60^o$ for various foundation gradient indices and are shown in Fig.7. It is seen from this figure that the radial displacement has compressed more than the other displacement components due to exerting the shear traction on the upper surface of the plate and normal interaction by the supporting foundation at the lower surface of the plate. The displacement U and stress σ_ξ (compression stress) increase and V, W, σ_Θ, $\tau_{\eta\theta}$, the maximum point of $\tau_{\theta\xi}$ decrease through the thickness of the plate as f_1, f_2 increase. Variation of stress σ_η along the plate thickness is compression and tension for small and large values of foundation gradient indices respectively and increases with increasing of f_1, f_2. The stress $\tau_{\eta\xi}$ is independent from Variations of foundation gradient indices.

Finally, influence of the various patterns of the stiffness variations on the static behavior of the plate (clamped supported) is investigated and the achieved results are presented in Fig.8. The foundation coefficients variation patterns are: uniform $f_1 = f_2 = 0$, linear $f_1 \neq 0, f_2 = 0$, parabolic $f_1 = 0, f_2 \neq 0$ and quadratic $f_1 \neq 0, f_2 \neq 0$. It can be found from Fig.8 that the linear stiffness variation lead to smaller U, σ_ξ and for other displacement and stress components the quadratic type of stiffness variation lead to smaller values, therefore this pattern has a higher load carrying contribution.

Fig.9 displays the effect of various parameters on clamped-clamped annular plate deflection. It is evident from Fig. 9 that the plate deflection decreases as gradient indices (n_1, n_2), foundation

coefficients (k_1, k_2), geometry non-uniformity coefficients (α_1, α_2) and foundation non-uniformity coefficients (f_1, f_2) increase.

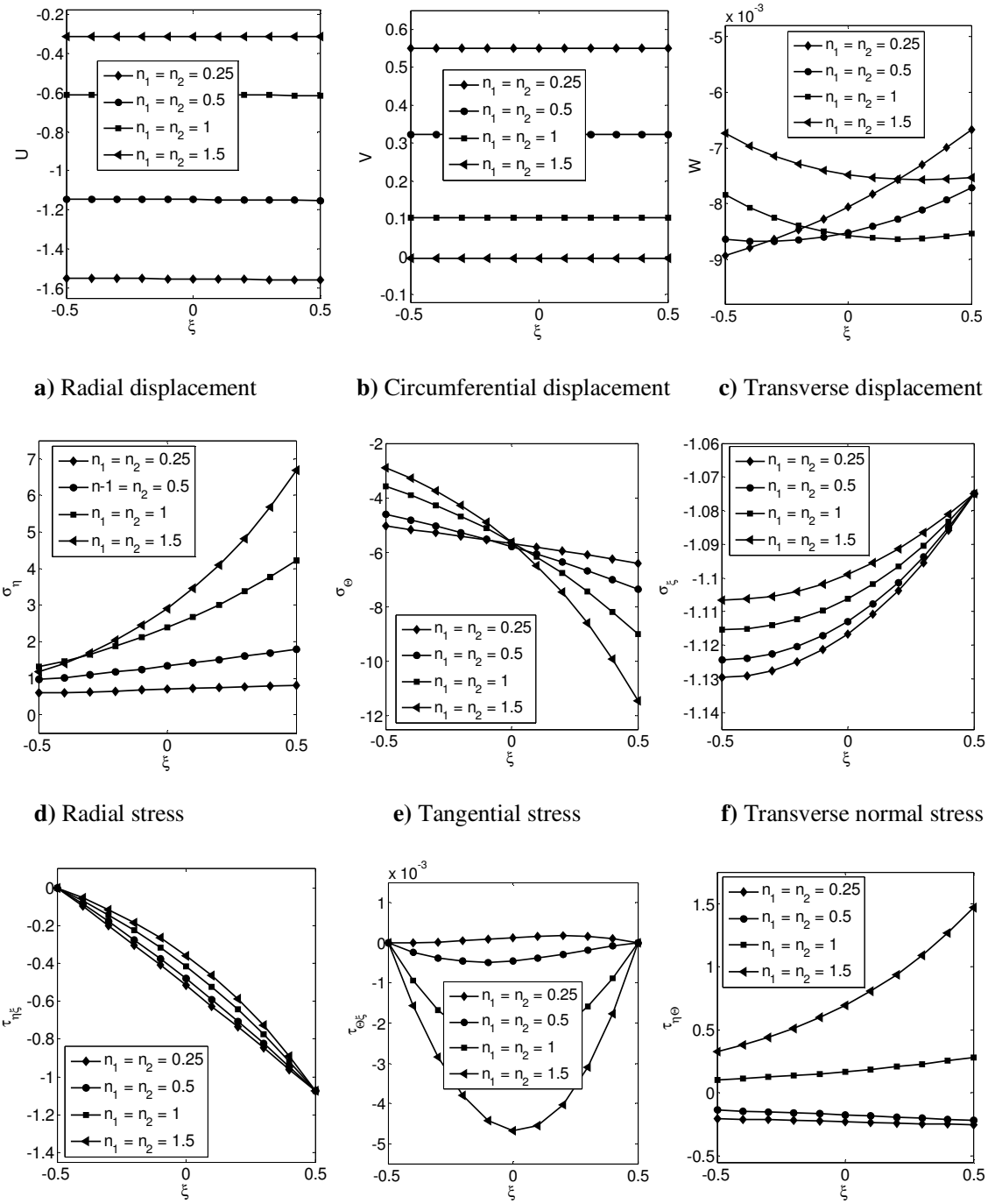

a) Radial displacement **b)** Circumferential displacement **c)** Transverse displacement

d) Radial stress **e)** Tangential stress **f)** Transverse normal stress

i) Tangential shear stress **h)** Transverse shear stress **g)** Transverse shear stress

Fig.4 Effect of the material heterogeneity indices on physical quantities across the plate thickness

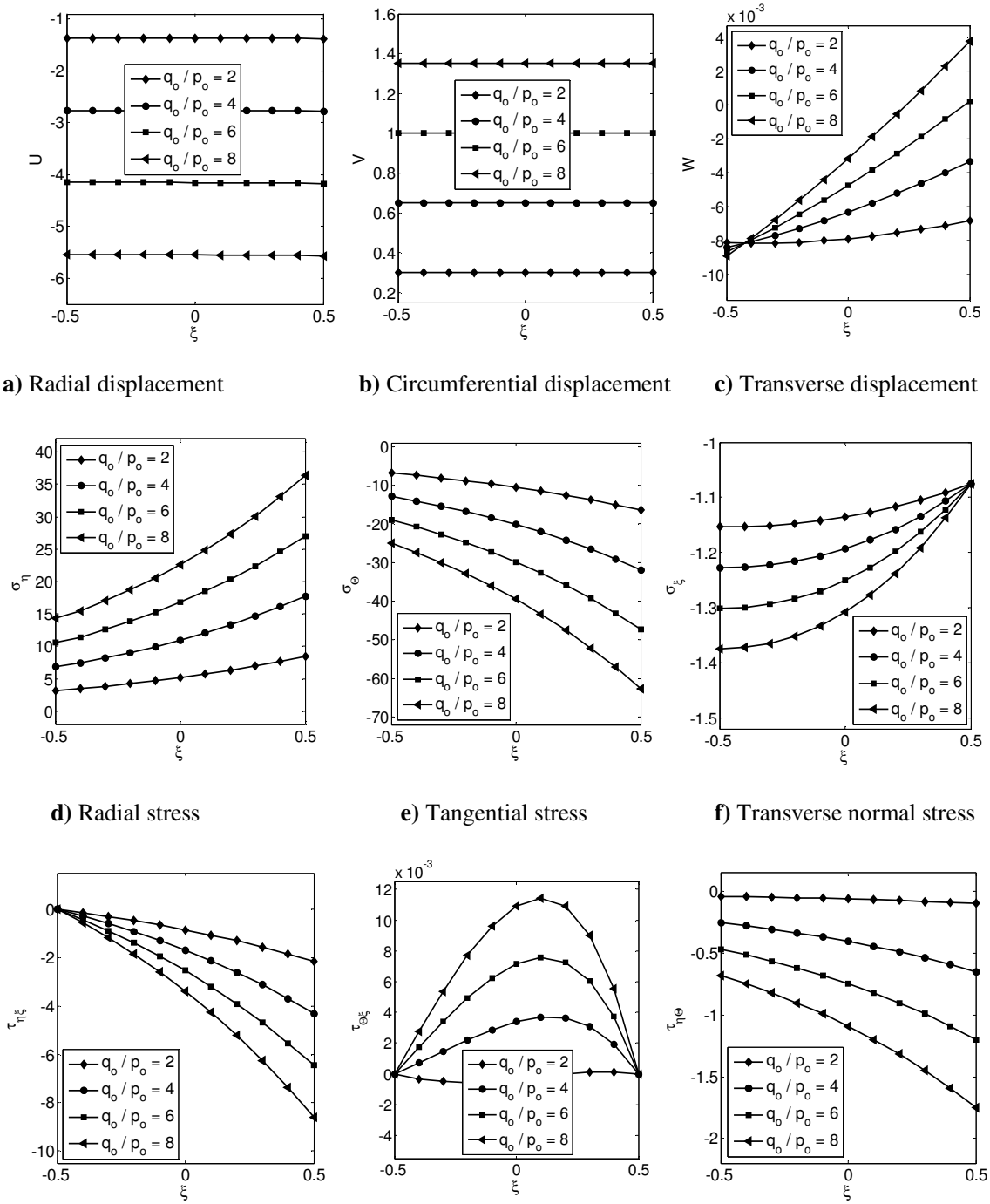

a) Radial displacement **b)** Circumferential displacement **c)** Transverse displacement

d) Radial stress **e)** Tangential stress **f)** Transverse normal stress

i) Tangential shear stress **h)** Transverse shear stress **g)** Transverse shear stress

Fig.5 Effect of the loads ratio on variation of mechanical entities across the plate thickness

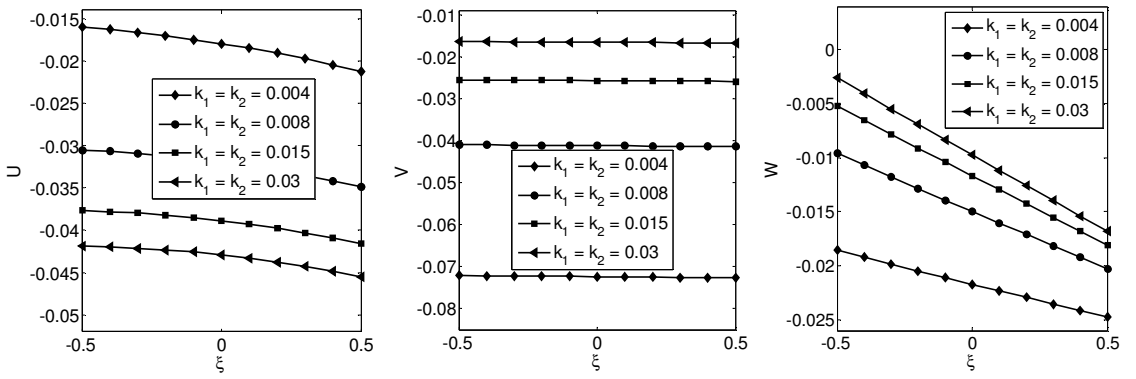

a) Radial displacement **b)** Circumferential displacement **c)** Transverse displacement

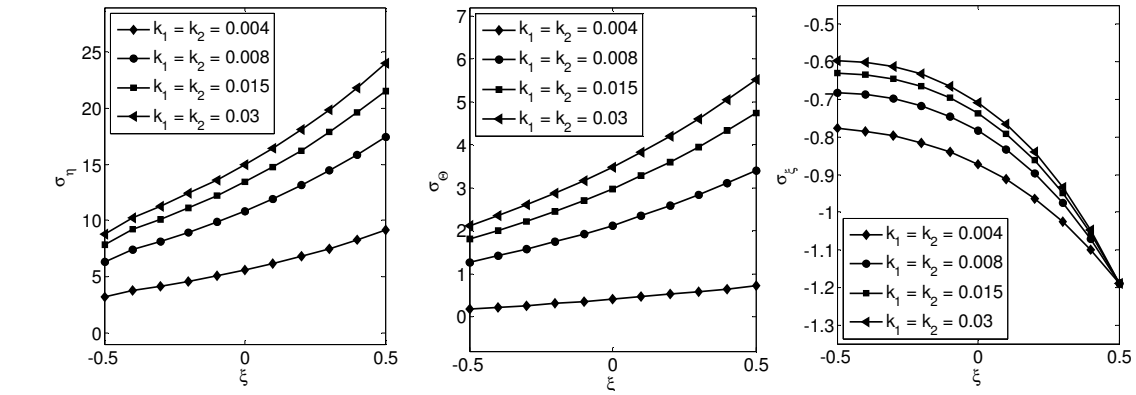

f) Transverse normal stress **e)** Tangential stress **d)** Radial stress

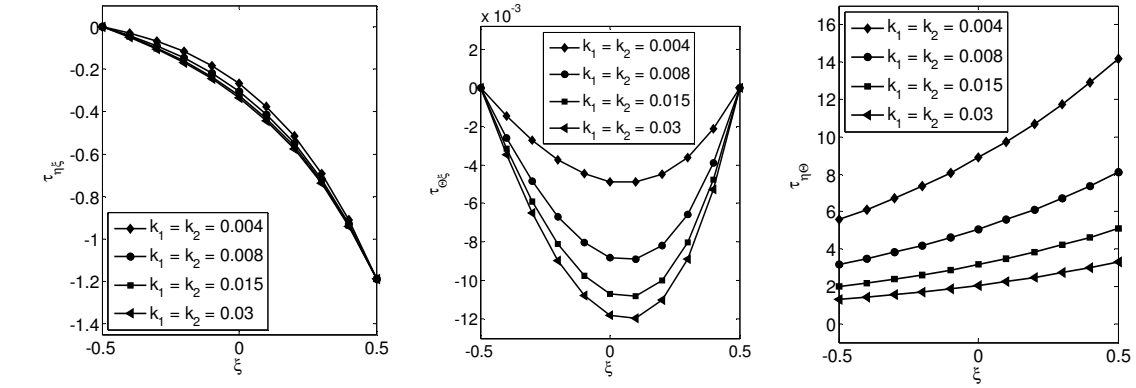

i) Tangential shear stress **h)** Transverse shear stress **g)** Transverse shear stress

Fig.6 Effect of the foundation coefficients on variation of mechanical entities across the plate thickness

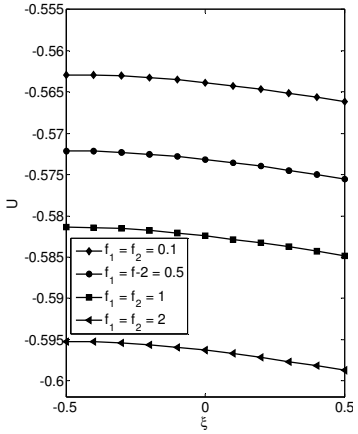

a) Radial displacement

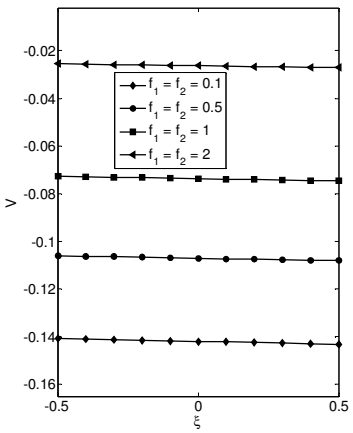

b) Circumferential displacement

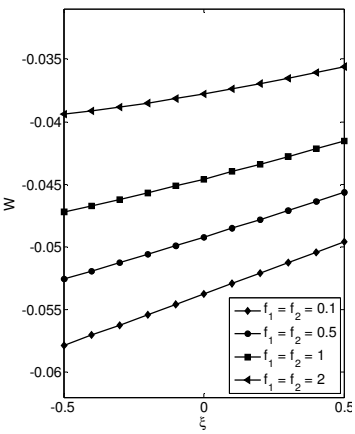

c) Transverse displacement

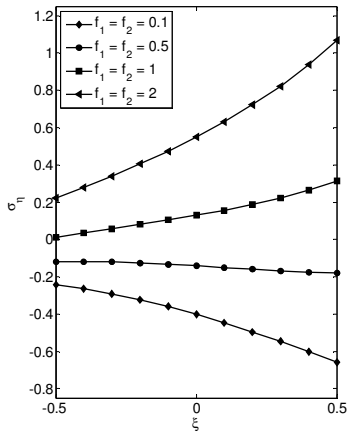

d) Radial stress

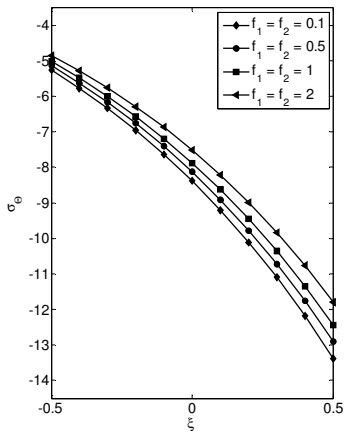

e) Tangential stress

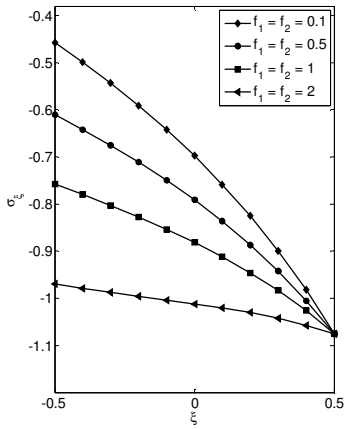

f) Transverse normal stress

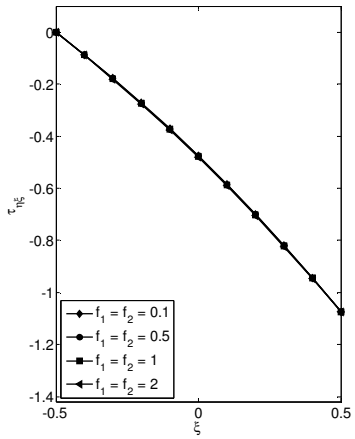

i) Tangential shear stress

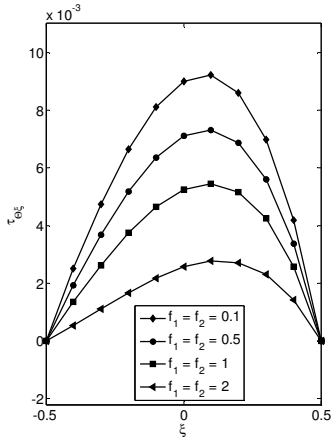

h) Transverse shear stress

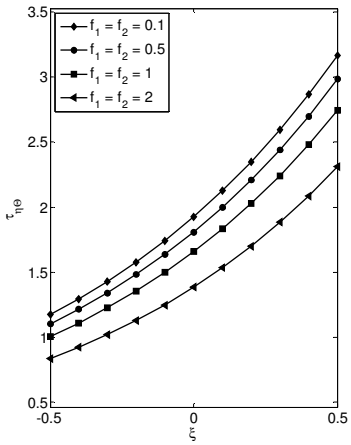

g) Transverse shear stress

Fig.7 Effect of foundation gradient indices on variation of mechanical entities across the plate thickness for a clamped circular plate

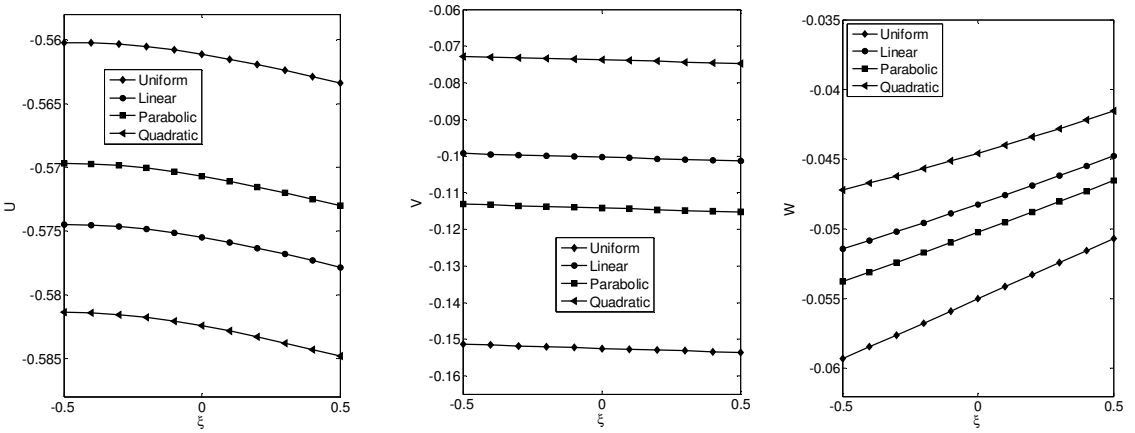

a) Radial displacement **b)** Circumferential displacement **c)** Transverse displacement

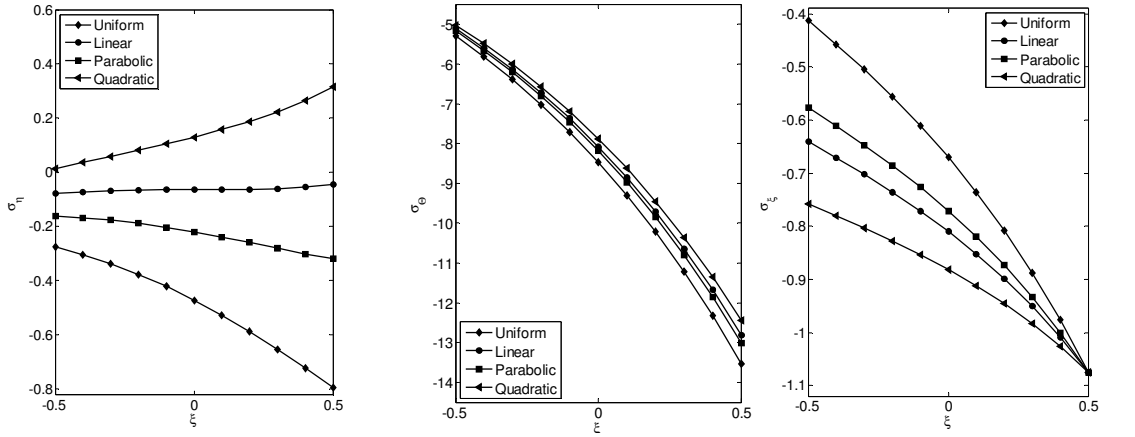

d) Radial stress **e)** Tangential stress **f)** Transverse normal stress

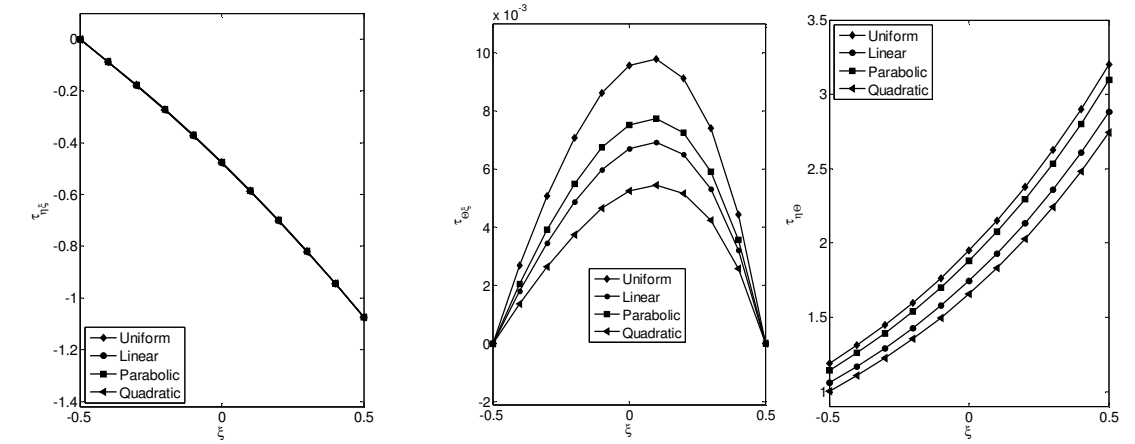

g) Transverse shear stress **h)** Transverse shear stress **i)** Tangential shear stress

Fig.8 Effect of various foundation patterns on variation of mechanical entities across the thickness direction for a clamped circular plate

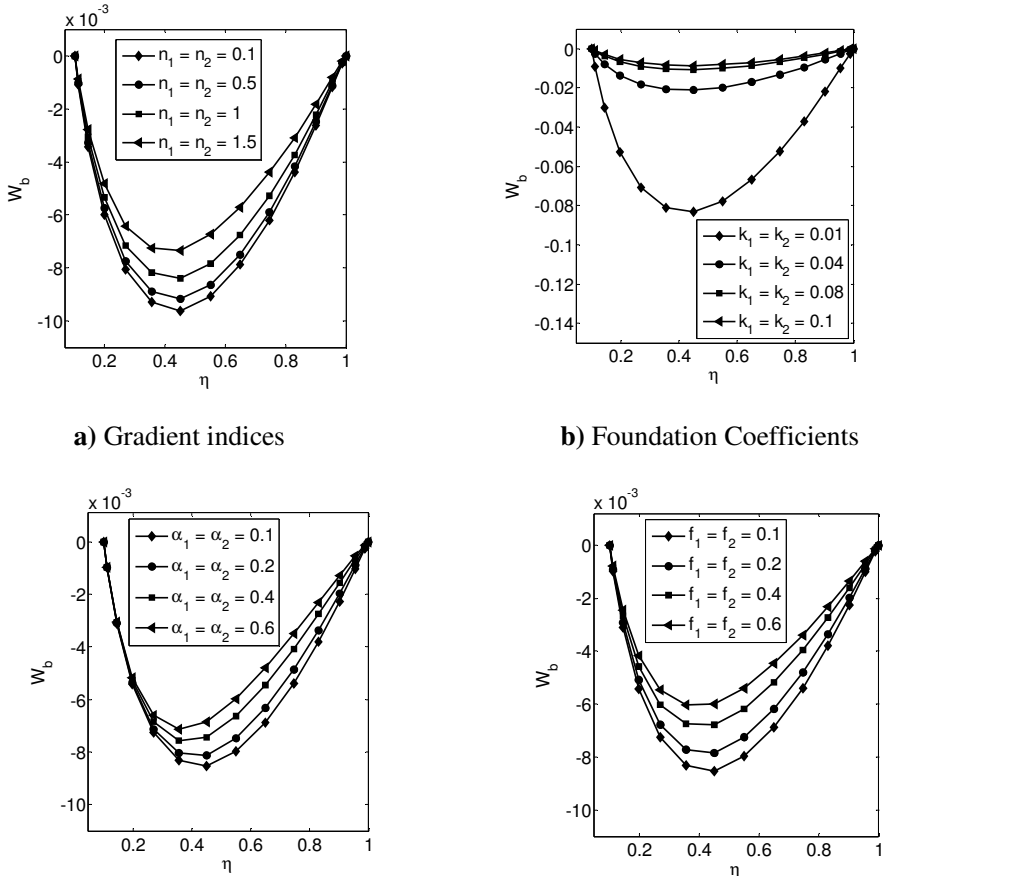

a) Gradient indices

b) Foundation Coefficients

c) Geometry non-uniformity Coefficients

d) Foundation non-uniformity Coefficients

Fig.9 Effect of various parameters on plate deflection at a location ($\theta = 45^{\circ}$)

5. Conclusions

In the present paper, the static behavior of variable thickness two directional functionally graded circular plates under non-uniform asymmetric boundary conditions is investigated based on three dimensional theory of elasticity. The material properties are assumed to vary exponentially in both thickness and radial directions. The solution is obtained by employing the semi-analytical method. The results confirm the high rate convergence and accuracy of the present method. Based on the results and discussions presented in this paper, the following important conclusions may be drawn.

- The presented method is especially useful to analysis the behavior of multi directional heterogeneous plates with a more complicated geometry and boundary conditions.
- The additional compression of the layers in the radial direction of the plate due to shear traction increases the radial and circumferential stresses.
- The rigidity of the plate increases with the increasing of elastic foundation coefficients.
- The additional compression of the radial displacement due to shear traction increases the surface buckling of the plate.
- Distribution of $\tau_{\eta\xi}$ along the plate thickness direction is independent from variations of foundation graded indices and stiffness gradient patterns.

- Load carrying contribution of quadratic type stiffness variation foundation is higher than the other stiffness variation patterns.
- The three dimensional theory presents an accurate prediction of three-axes Von-Misses stress, and as a result, it can accurately estimate the structure strength.

APPENDIX 1

The elements of state matrix at discretized points are

$$D_i=\begin{bmatrix} [0]_{N\times N} & [0]_{N\times N} & [0]_{N\times N} & [\delta_{ij}]_{N\times N} & [0]_{N\times N} & [0]_{N\times N} \\ [0]_{N\times N} & [0]_{N\times N} & [0]_{N\times N} & [0]_{N\times N} & [\delta_{ij}]_{N\times N} & [0]_{N\times N} \\ [0]_{N\times N} & [0]_{N\times N} & [0]_{N\times N} & [0]_{N\times N} & [0]_{N\times N} & [\delta_{ij}]_{N\times N} \\ [d_{ij}^{41}]_{N\times N} & [d_{ij}^{42}]_{N\times N} & [d_{ij}^{43}]_{N\times N} & [d_{ij}^{44}]_{N\times N} & [d_{ij}^{45}]_{N\times N} & [d_{ij}^{46}]_{N\times N} \\ [d_{ij}^{51}]_{N\times N} & [d_{ij}^{52}]_{N\times N} & [d_{ij}^{53}]_{N\times N} & [d_{ij}^{54}]_{N\times N} & [d_{ij}^{55}]_{N\times N} & [d_{ij}^{56}]_{N\times N} \\ [d_{ij}^{61}]_{N\times N} & [d_{ij}^{62}]_{N\times N} & [d_{ij}^{63}]_{N\times N} & [d_{ij}^{64}]_{N\times N} & [d_{ij}^{65}]_{N\times N} & [d_{ij}^{66}]_{N\times N} \end{bmatrix}_{6N\times 6N}$$

where $\delta_{ij}=0\ (i\neq j)\ ;\ \delta_{ii}=1$

$$d_{ii}^{41}=-\left(\frac{2(1-\nu)}{1-2\nu}\right)(s)^2\beta_{1i}^2\left(A_{ii}^{(2)}+\left(\frac{1}{\eta_i}+\frac{n_2}{1-b/a}+2\beta_{2i}\right)A_{ii}^{(1)}+\left((\frac{1}{\eta_i}+\frac{n_2}{1-b/a})\beta_{2i}+\beta_{3i}-\frac{1}{\eta_i^{\,2}}\right)\right)$$

$$-\left(\frac{2\nu}{(1-2\nu)}\right)(s)^2\beta_{1i}^2\frac{n_2}{\eta_i(1-b/a)}+(s)^2\beta_{1i}^2\frac{1}{\eta_i^2}\quad (i=j)$$

$$d_{ij}^{41}=-\left(\frac{2(1-\nu)}{1-2\nu}\right)(s)^2\beta_{1i}^2\left(\sum_{j=1}^{N}A_{ij}^{(2)}+\left(\frac{1}{\eta_i}+\frac{n_2}{1-b/a}+2\beta_{2i}\right)\sum_{j=1}^{N}A_{ii}^{(1)}\right)\quad (i\neq j)$$

$$d_{ii}^{42}=-\left(\frac{2\nu}{1-2\nu}\right)(s)^2\beta_{1i}^2\frac{1}{\eta_i}\left(A_{ii}^{(1)}+\left(\frac{n_2}{1-b/a}+\beta_{2i}\right)\right)+\left(\frac{2(1-\nu)}{(1-2\nu)}\right)(s)^2\beta_{1i}^2\frac{1}{\eta_i^2}$$

$$-(s)^2\beta_{1i}^2\left(\frac{1}{\eta_i}A_{ii}^{(1)}+\left(\frac{\beta_{2i}}{\eta_i}-\frac{1}{\eta_i^2}\right)\right)\quad (i=j)$$

$$d_{ij}^{42}=-\left(\frac{1}{1-2\nu}\right)(s)^2\beta_{1i}^2\frac{1}{\eta_i}\sum_{j=1}^{N}A_{ij}^{(1)}\quad (i\neq j)$$

$$d_{ii}^{43}=-n_1 s\beta_{1i}\left(A_{ii}^{(1)}+\beta_{2i}\right)\quad (i=j)\quad ,\quad d_{ij}^{43}=-n_1 s\beta_{1i}\sum_{j=1}^{N}A_{ij}^{(1)}\quad (i\neq j)$$

$$d_{ii}^{44}=-n_1,\ d_{ij}^{44}=0$$

$$d_{ii}^{46}=-\left(\frac{2\nu}{1-2\nu}\right)s\beta_{1i}\left(A_{ii}^{(1)}+\left(\beta_{2i}+\frac{n_2}{1-b/a}+\frac{1}{\eta_i}\right)\right)+\left(\frac{2\nu}{(1-2\nu)}\right)s\beta_{1i}\frac{1}{\eta_i}$$

$$-s\beta_{1i}\left(A_{ii}^{(1)}+\beta_{2i}\right)\quad (i=j)$$

$$d_{ij}^{46}=-\left(\frac{1}{1-2\nu}\right)s\beta_{1i}\sum_{j=1}^{N}A_{ij}^{(1)}\quad (i\neq j)$$

$$d_{ii}^{51}=\left(\frac{2\nu}{1-2\nu}\right)s^2\beta_{1i}^2\frac{1}{\eta_i}\left(A_{ii}^{(1)}+\beta_{2i}\right)+\left(\frac{2(1-\nu)}{(1-2\nu)}\right)s^2\beta_{1i}^2\frac{1}{\eta_i^2}$$

$$+s^2\beta_{1i}^2\left(\frac{1}{\eta_i}A_{ii}^{(1)}+\left(\frac{1}{\eta_i}\left(\beta_{2i}+\frac{n_2}{1-b/a}\right)+\frac{1}{\eta_i^2}\right)\right)\quad (i=j),\quad d_{ij}^{51}=\left(\frac{1}{1-2\nu}\right)s^2\beta_{1i}^2\frac{1}{\eta_i}\sum_{j=1}^{N}A_{ij}^{(1)}\quad (i\neq j)$$

$$d_{ii}^{52}=-s^2\beta_{1i}^2\left(A_{ii}^{(2)}+\left(2\beta_{2i}+\frac{1}{\eta_i}+\frac{n_2}{1-b/a}\right)A_{ii}^{(1)}+\left(\beta_{2i}+\beta_{3i}+\left(\beta_{2i}-\frac{1}{\eta_i}\right)\frac{n_2}{1-b/a}-\frac{1}{\eta_i^2}\right)\right)$$

$$+\left(\frac{2(1-\nu)}{1-2\nu}\right)s^2\beta_{1i}^2\frac{1}{\eta_i^2}\qquad (i=j)$$

$$d_{ij}^{52}=-s^2\beta_{1i}^2\left(\sum_{j=1}^{N}A_{ij}^{(2)}+\left(2\beta_{2i}+\frac{1}{\eta_i}+\frac{n_2}{1-b/a}\right)\sum_{j=1}^{N}A_{ij}^{(1)}\right)\quad (i\neq j)$$

$$d_{ii}^{53}=-n_1 s\beta_{1i}\frac{1}{\eta_i}\quad (i=j)\quad ,\quad d_{ij}^{53}=0\quad (i\neq j)$$

$$d_{ii}^{55}=-n_1\quad (i=j)\quad ,\quad d_{ij}^{55}=0\quad (i\neq j)$$

$$d_{ii}^{56}=-\frac{1}{\eta_i}\left(\frac{1}{1-2\nu}\right)\quad (i=j)\quad ,\quad d_{ij}^{56}=0\quad (i\neq j)$$

$$d_{ii}^{61}=-n_1\left(\frac{\nu}{1-\nu}\right)s\beta_{1i}\left(A_{ii}+\left(\beta_{2i}+\frac{1}{\eta_i}\right)\right)\quad (i=j),\quad d_{ij}^{61}=-n_1\left(\frac{\nu}{1-\nu}\right)s\beta_{1i}\sum_{j=1}^{N}A_{ij}\quad (i\neq j)$$

$$d_{ii}^{62}=-n_1\left(\frac{\nu}{1-\nu}\right)s\beta_{1i}\frac{1}{\eta_i}\quad (i=j),\quad d_{ij}^{62}=0\quad (i\neq j)$$

$$d_{ii}^{63}=-\left(\frac{1-2\nu}{2(1-2\nu)}\right)s^2\beta_{1i}^2\left(A_{ii}^{(2)}+\left(\frac{1}{\eta_i}+2\beta_{2i}+\frac{n_2}{1-b/a}\right)A_{ii}^{(1)}+\left(\beta_{3i}+\beta_{2i}(\frac{1}{\eta_i}+\frac{n_2}{1-b/a})\right)\right)\quad (i=j)$$

$$d_{ij}^{63}=-\left(\frac{1-2\nu}{2(1-2\nu)}\right)s^2\beta_{1i}^2\left(\sum_{j=1}^{N}A_{ij}^{(2)}+\left(\frac{1}{\eta_i}+2\beta_{2i}+\frac{n_2}{1-b/a}\right)\sum_{j=1}^{N}A_{ij}^{(1)}\right)\quad (i\neq j)$$

$$d_{ii}^{64}=-\left(\frac{\nu}{(1-\nu)}\right)s\beta_{1i}\left(A_{ii}+\frac{1}{\eta_i}\left(\beta_{2i}+\frac{1}{\eta_i}\right)\right)-\left(\frac{1-2\nu}{2(1-\nu)}\right)s\beta_{1i}\left(\frac{n_2}{1-b/a}\right)\quad (i=j)$$

$$d_{ij}^{64}=-\left(\frac{\nu}{(1-\nu)}\right)s\beta_{1i}\sum_{j=1}^{N}A_{ij}^{(1)}\quad (i\neq j)$$

$$d_{ii}^{65}=-\frac{1}{2(1-\nu)}\frac{s\beta_{1i}}{\eta_i}\quad (i=j),\ d_{ij}^{65}=0\quad (i\neq j)$$

$$d_{ii}^{66}=-n_1\quad (i=j),\ d_{ij}^{66}=0\quad (i\neq j)$$

i,j = 1,2,3, … , N (A1)

References

[1]Nemat-Alla M. Reduction of thermal stresses by developing two-dimensional functionally graded materials, Int. J. Solids Struct., 40, 7339-7356 (2003).

[2]Saidi AR, Rasouli A, Sahraee S. Axisymmetric bending and buckling analysis of thick functionally graded circular plates using unconstrained third-order shear deformation plate theory. Compos Struct., 89(1):110–9 (2009).

[3]Nosier A., Fallah F., Non-linear analysis of functionally graded circular plates under asymmetric transverse loading, Int. J. Non-linear Mech., 44, 928-942 (2009).

[4]Sahraee S, Saidi AR. Axisymmetric bending analysis of thick functionally graded circular plates using fourth-order shear deformation theory. Eur. J Mech. A/Solids 28(5):974–84 (2009).

[5]Malekzadeh P., Golbahar Haghighi M.R., Atashi M.M., Free vibration analysis of elastically supported functionally graded annular plates subjected to thermal environment, meccanica, 47(2), 321-333 (2011).

[6]Safaeian Hamzehkolaei N., Malekzadeh P., Vaseghi J, Thermal effect on axisymmetric bending of functionally graded circular and annular plates using DQM, Steel Compos. Struct., 11(4), 341-358(2011).

[7]Kumar Y., Lal R., prediction of frequencies of free axisymmetric vibration of two directional functionally graded annular plates on Winkler foundation, Eur. J. Mech. A-Solid., 42, 219-228 (2013).

[8]Shariyat M., Alipour M.M., Differential transform vibration and modal stress analyses of circular plates made of two-directional functionally graded materials resting on elastic foundations, Arch. Appl. Mech., 81(9), 1289-1306 (2011).

[9]Abbasi S., Farhatnia F., Jazi SR., A semi-analytical solution on static analysis of circular plate exposed to non-uniform axisymmetric transverse loading resting on Winkler elastic foundation, Archives of Civil and Mechanical Engineering, DOI: 10.1016/ j. acme. 2013.09.007.

[10] Li XY., Ding HJ. , Chen W.Q., Elasticity solutions for a transversely isotropic functionally graded circular plate subject to an axisymmetric transverse load $q r^k$, Int. J. Solids Struct., 45(1), 191–210 (2008).

[11] Wang, Y, Xu, RQ, and Ding, HJ. Three-dimensional solution of axisymmetric bending of functionally graded circular plates, Compos. Struct., 92: 1683–1693 (2010).

[12] Yun W., Rongqiao X., Haojiang D., Three-dimensional solution of axisymmetric bending of functionally graded circular plates, Compos. Struct., 92, 1683-1693 (2010).

[13] Sburlati R., Bardella L., Three-dimensional elastic solutions for functionally graded circular plates, Eur. J. Mech. A-Solid., 30, 219-235 (2011).

[14] Nie GJ. , Zhong Z., Axisymmetric bending of two-directional functionally graded circular and annular plates. Acta Mech. Solid Sin., 20(4), 289-295 (2007).

[15] Lu C.F., Lim C.W., Chen W.Q., Semi-analytical analysis for multi-directional functionally graded plates: 3-D elasticity solutions, Int. J. Num. Meth. Eng., 79, 25 – 44 (2009).

[16] Davoodi K. I., Ghayour M., Mirdamadi H. R., Free vibration analysis of multi-directional functionally graded circular and annular plates, Mech. Sci. Tech., 26(11), 3399-3410, 2012.

[17] Behravan Rad A., Semi-analytical solution for functionally graded solid circular and annular plates resting on elastic foundations subjected to axisymmetric transverse loading, Adv. Appl. Math. Mech., 4(2), 205 – 222, 2012.

[18] Behravan Rad A., Alibeigloo A., Semi-analytical solution for the static analysis of 2D functionally graded circular and annular circular plates resting on elastic foundation, Mech. Adv. Mat. Struc. 20(7), 515-528, 2013.

[19] Shu, C., Differential Quadrature and Its Application in Engineering, Springer, New York, (2000).

[20] Zong Z., Zhang Y., Advanced Differential Quadrature Methods. CRC Press, New York, (2009).